ELSEVIER

Ceramics International 27 (2001) 501–507

CERAMICS INTERNATIONAL

www.elsevier.com/locate/ceramint

Influence of the total fines content on the thermal shock damage resistance of Al_2O_3–spinel castables

Yung-Chao Ko *

China Steel Corporation, Kaohsiung, Taiwan, Republic of China

Received 28 August 2000; received in revised form 12 September 2000; accepted 19 September 2000

Abstract

The thermal shock damage resistance of Al_2O_3–spinel castables containing 18 wt.% -30 + 10 mm top size aggregates with 31–41 wt.% -0.075 mm total fines and 6 wt.% -8 + 5 mm top size aggregates with 35 wt.% -0.075 mm total fines was investigated using the prism quench into water technique. Experimental results indicated that castables containing no more than 35 wt.% -0.075 mm total fines have better thermal shock damage resistance, regardless of the size and amount of the top size aggregates. The thermal shock damage resistance parameters, R'''' and R_{st}, can be linearly correlated with the retained strength of castables, which increases with an increase in the magnitudes of R'''' and R_{st}.

Keywords: C. Thermal shock damage resistance; Total fines content

1. Introduction

Both practice and theory [1,2] show that the thermal shock damage resistance of refractories can be improved to some extent by using larger size aggregates. The previous study [3] found that the thermal shock resistance of the gap-sized castables is superior to that of the continuous-sized castables; the thermal shock damage resistance parameter, R'''' can be linearly correlated with the trends, while the thermal shock damage resistance parameter, R_{st}, was found to be inversely related to the trends. The latest studies [4,5] on the thermal shock resistance of castable specimens after the panel spalling test indicated that in fine grain castables cracks propagate almost straightly, while in coarse grain castables cracks tend to be deflected or branched from the coarse aggregates; there is an optimum amount of top size aggregates for thermal shock resistance enhancement; and the optimum amount of top size aggregates for improving the thermal shock resistance of castables decreases with a decrease in top size.

It seems that all the attention was drawn to the importance of aggregate size distribution and the amount of top size aggregates for thermal shock resistance considerations with little attention directed toward the total fines content of castables. The purpose of the present work is to investigate the influence of the total fines content on the thermal shock resistance of Al_2O_3–spinel castables.

2. Experimental procedures

2.1. Materials

The chemical composition of the raw materials is given in Table 1. The constituents of castables are listed in Table 2. The sieve analyses of castables are shown in Table 3. The selection of total fines content varing from 30 to 40 wt.% is to reflect the total fines content fluctuation in commercial castables which greatly affects the performance in the field.

2.2. Procedures

2.2.1. Specimen preparation and thermal shock damage test

These castables were cast with water (6.5 wt.% solids) using sodium polymethacrylate (0.1 wt.% solids) as a deflocculant with the aid of a vibrating table. Castables were cured in air at 28–30°C ambient temperature for 24 h and then dried at 110°C for at least 16 h before firing. Specimens 160 by 40 by 40 mm were cast for measuring

* Tel.: +886-07-8021111.

0272-8842/01/$20.00
PII: S0272-8842(00)00102-4

Table 1
Chemical analyses of raw materials

Type	Composition (wt.%)						
	Al_2O_3	SiO_2	Fe_2O_3	TiO_2	Na_2O	MgO	CaO
White fused alumina	99.7	0.016	0.013	0.004	0.15	–	–
Calcined alumina	99.7	0.02	0.01	–	0.27	–	–
Reactive alumina	99.6	0.02	0.01	–	0.26	–	–
Calcined spinel	89.4	0.1	0.1	–	–	10.0	0.1
Calcined spinel	94.1	0.05	0.05	–	–	5.41	0.29
Cement	80.0	0.08	0.08	< 0.01	–	0.08	17.2

the physical properties. Physical properties such as apparent porosity, bulk density and cold modulus of rupture of the castables fired at 1500°C for 3 h were measured according to JIS [6]. Each properties measurement was determined using three specimens.

The thermal shock damage test was conducted by quenching a specimen into 25°C water. Prior to quenching each specimen was heated at 1500°C for 3 h, followed by overnight furnace cooling. One prism quench cycle consisted of reheating a specimen at 1100°C for 1 h, followed by quenching into a 25°C water barrel.

2.2.2. Physical properties measurements for the determination of thermal shock damage parameters

Specimens for measuring modulus of rupture (σ_f), Young's modulus (E), notched beam fracture surface energy (γ_{NBT}) and work of fracture surface energy (γ_{WOF}) for calculating the thermal shock damage resistance parameters R'''' and R_{st} were cut from a cast 140 by 160 by 40 mm whose top surface was ground with a diamond wheel for flatness. Prior to the cut , all of the casts were heated at 1500°C for 3 h.

γ_{NBT} and γ_{WOF} were measured by the notched beam test and the work of fracture methods [7,8], respectively. Specimen configurations and notch geometries are shown in Fig. 1 [7]. The required notches were cut with a 3-mm thick diamond blade.

γ_{NBT} was calculating from the equation [7] using Poisson ratio 0.18:

$$\gamma_{NBT} = \frac{9P^2L^2C(1-\nu^2)}{8W^2D^4E}\left[A_0 + A_1\left(\frac{C}{D}\right) + A_2\left(\frac{C}{D}\right)^2 + A_3\left(\frac{C}{D}\right)^3 + A_4\left(\frac{C}{D}\right)^4\right]^2$$

Table 2
Constituents and main-chemical composition of castables

Castable type	Constituent (wt.%)			Composition (wt.%)		
	Alumina	Spinel	Cement	Al_2O_3	MgO	CaO
Top size 18%-30 + 10 mm fines 35%-0.075 mm	83.5	10.0[a]	6.5	97.38	1.0	1.12
Top size 6%-8 + 5 mm fines 35%-0.075 mm	83.5	10.0[a]	6.5	97.38	1.0	1.12
Top size 18%-30 + 10 mm fines 41%-0.075 mm	71.5	18.5[b]	10.0	96.78	1.0	1.72
Top size 18%-30 + 10 mm fines 31%-0.075 mm	71.5	18.5[b]	10.0	96.78	1.0	1.72

[a] Spinel containing 10 wt.% MgO.
[b] Spinel containing 5.41 wt.% MgO.

Table 3
Sieve analyses of castables

Castable type	Retained on sieve[a] (wt.%)					
	$\frac{-30}{+10}$	$\frac{-8}{+5}$	$\frac{-5}{+3}$	$\frac{-3}{+1}$	$\frac{-1}{+0.075}$	−0.075
Top size 18%-30 + 10 mm fines 35%-0.075 mm	18	2	9	22	14	35
Top size 6%-8 + 5mm fines 35%-0.075 mm	–	6	16	26	17	35
Top size 18%-30 + 10 mm fines 41%-0.075 mm	18	2	11	21	7	41
Top size 18%-30 + 10 mm fines 31%-0.075 mm	18	2	11	21	17	31

[a] Sieve openings given in mm.

where P is the load at failure, L is the span, D and W are specimen thickness and width, respectively, and C is the notch depth, with $C \approx \frac{D}{2}$, $A_0 = 1.90 + 0.0075(L/D)$, $A_1 = -3.39 + 0.08(L/D)$, $A_2 = 15.4 - 0.2175(L/D)$, $A_3 = -26.24 + 0.2815(L/D)$, $A_4 = 26.28 - 0.145(L/D)$, ν is Poisson ratio and E is Young's modulus.

$\gamma_{WOF=\int Pdx/2A}$, where $\int Pdx$ is the area under the load–deflection curve and A is the projected area of each of the newly formed fracture surface.

σ_f, γ_{NBT} and γ_{WOF} of the castables fired at 1500°C for 3 h were measured at 25°C ambient temperature in a 3-point bending on 100 mm span. γ_{NBT} and γ_{WOF} were measured at a crosshead speed of 1.25 and 0.05 mm min^{-1}, respectively [3]. σ_f was measured at a crosshead speed of 0.125 mm min^{-1} [9]. E was determined using the sonic method [10]. Each property measurement was determined using three specimens.

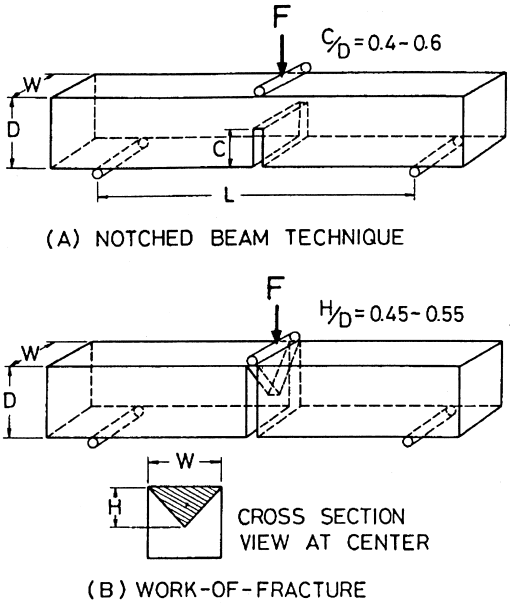

Fig. 1. Specimen configurations and notch geometries (after Ref. 7).

2.3. Equipment

The testing machine was MTS model number 10/GL and the software used for the determination of σ_f and γ_{WOF} was Teamwork 3.0.

3. Results and discussion

3.1. Physical properties variation

3.1.1. Porosity and thermal expansion coefficient

Tables 2 and 4 show that the porosity of Al_2O_3–spinel castables slightly increased with an increase in cement content. The thermal expansion coefficient of Al_2O_3–spinel castables slightly increases with an increase in MgO content [11]. All of the castables in the present work contained 1 wt.% MgO, based on Tables 1 and 2. Hence, the thermal expansion coefficient difference is due to the cement content difference as shown in Tables 2 and 4.

3.1.2. Modulus of rupture and Young's modulus

As can be seen from Table 4, porosity increased from 23 to 24%, while modulus of rupture increased from 8.5 to 13 MPa and Young's modulus increased from 53 to 61 GPa.

Chan et al. [12] and Ko et al. [13] observed the growth of some CA_6 crystals out of the Al_2O_3-rich spinel grain in the bonding matrix of the castables fired at 1500°C for 3 h and concluded the bond linkage between CA_6 and spinel grains responsible for the hot strength increase with an increase in either CaO or spinel, and temperature from 1300 to 1500°C.

As shown in Table 2, the castables of top size −30 + 10 mm with 31 wt.% -0.075 mm fines and the castables of top size −30 + 10 mm with 41 wt.% -0.075 mm fines contained 1.72 wt.% CaO and 18.5 wt.% spinel, while the castables of top size −30 + 10 mm with 35 wt.% -0.075 mm fines and the castables of top size

Table 4
Physical properties of castables

Castable type	Apparent porosity (%)	Bulk density (g/cm^3)	Modulus of rupture (MPa)	Young's modulus (GPa)	Thermal expansion coefficient ($°C^{-1}$)
Top size 18%-30 + 10 mm fines 35%-0.075 mm	23.1	2.98	8.42±0.45	53.2±3.6	8.0×10^{-6}
Top size 6%-8 + 5 mm fines 35%-0.075 mm	23.3	2.99	8.51±1.62	53.5±5.5	8.0×10^{-6}
Top size 18%-30 + 10 mm fines 41%-0.075 mm	24.3	2.93	13.61±1.28	60.9±1.8	8.5×10^{-6}
Top size 18%-30 + 10 mm fines 31%-0.075 mm	24.2	2.93	12.08±0.80	61.9±3.0	8.5×10^{-6}

Table 5
Fracture surface energies and thermal shock damage data of castables[a]

Castable type	γ_{WOF} (J/m^2)	γ_{NBT} (J/m^2)	R''''' (cm)	R_{st} (cm$^{1/2}$C)	Retained strength (%)	
					One-quench	Three-quench
Top size 18%-30 + 10 mm fines 35%-0.075 mm	61.03±13.85	12.82±5.65	4.58	42.34	41	29
Top size 6%-8 + 5 mm fines 35%-0.075 mm	59.54±7.30	7.42±1.49	4.40	41.70	36	27
Top size 18%-30 + 10 mm fines 41%-0.075 mm	74.90±10.02	12.72±2.91	2.46	41.26	28	18
Top size 18%-30 + 10 mm fines 31%-0.075 mm	78.44±8.14	11.71±1.21	3.33	41.88	33	28

[a] Quenching at the temperature difference $\Delta T = 1100$°C.

−8 + 5 mm with 35 wt.% -0.075 mm fines contained 1.12 wt.% CaO and 10 wt.% spinel. The former contain more CaO and more spinel than the latter. This explains why the former have greater magnitudes of modulus of rupture and Young's modulus than the latter as shown in Table 4. Although the castables containing 18.5 wt.% spinel of 95 wt.% Al_2O_3 and those of 10 wt.% spinel of 90 wt.% Al_2O_3 have the same amount of MgO, the castables of higher spinel content have more spinel sites, which contribute more to bonding strength.

3.2. Fracture surface energies

Plots of work of fracture surface energy against both Young's modulus and modulus of ruptuer, based on the data as shown in Tables 4 and 5, indicate that the work of fracture can be linearly correlated with both Young's modulus and modulus of rupture as shown in Figs. 2 and 3. The magnitudes of work of fracture increase with an increase in both Young's modulus and modulus of rupture.

The work of fracture is a measure of the total energy dissipated during fracture and the increase in work of fracture is a consequence of an increased degree of microcracking and the formation of more tortuous fracture paths [3]. It is believed that a high strength bonding matrix of castables is required for enhancing the magnitude of work of fracture surface energy.

The notched beam fracture surface energy is a measure of the energy necessary to initiate movement of a pre-existing flaw [3]. As can be seen from Table 5, the magnitudes of notched beam fracture surface energies of castables of top size −30 + 10 mm nearly remain constant at 12 J/m^2, while that of castables of top size −8 + 5 mm is 7 J/m^2. Apparently the magnitudes of notched beam fracture surface energy of castables are dictated by the size and amount of top size aggregates. The present work indicates that fracture initiation is a much easier process in the castables containing a smaller size and a less amount of top size aggregates.

3.3. Thermal shock damage behavior

Table 6 gives the strength degradation of castables after prism quench tests. Figs. 4 and 5 show the typical variation of retained strength with prism quench cycles. According to Homeny et al. [3], strength degradation of castables generally levels off after 3–5 cycles. It is believed that a fairly accurate strength degradation can be obtained after three quench cycles to provide a basis for comparison. The relationship between retained strength and total fines content of castables is shown in Fig. 6. Castables containing no more than 35 wt.% -0.075 mm fines generally have a higher percentage retained strength than those containing 41 wt.% −0.075 mm fines, regardless of the size and amount of top size aggregates after one-quench and three-quench tests. It is

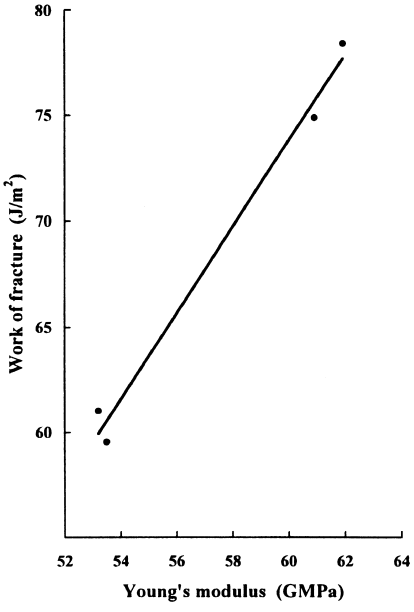

Fig. 2. Variation of work of fracture surface energy with Young's modulus of castables.

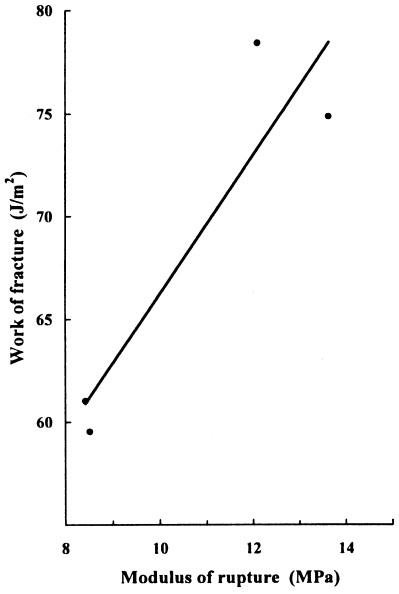

Fig. 3. Variation of work of fracture surface energy with modulus of rupture of castables.

Table 6
Strength degradation of castables after quench into 25°C water

Castable type	Modulus of rupture (MPa)[a]		
	Furnace cooling	One-quench	Three-quench
Top size 18%-30+10 mm fines 35%-0.075 mm	15±0.3	6.2±1.0	4.3±0.3
Top size 6%-8+5 mm fines 35%-0.075 mm	17±0.4	6.1±0.2	4.5±0.8
Top size 18%-30+10 mm fines 41%-0.075 mm	21±0.1	5.9±0.4	3.9±1.6
Top size 18%-30+10 mm fines 31%-0.075 mm	18±1.9	6.0±1.5	5.1±0.6

[a] Strength was determined in accordance with JIS (Ref. 6).

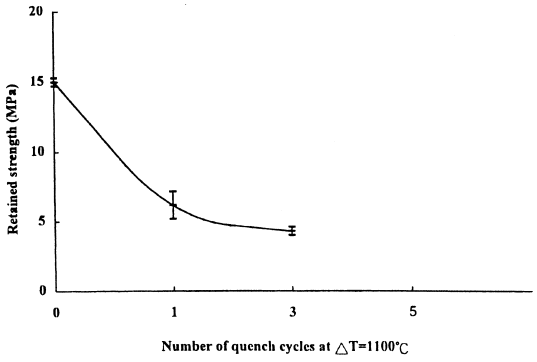

Fig. 4. Variation of retained strength with the water quench cycle of castables containing 18 wt.% -30+10 mm top size aggregates with 35 wt.% -0.075 mm fines.

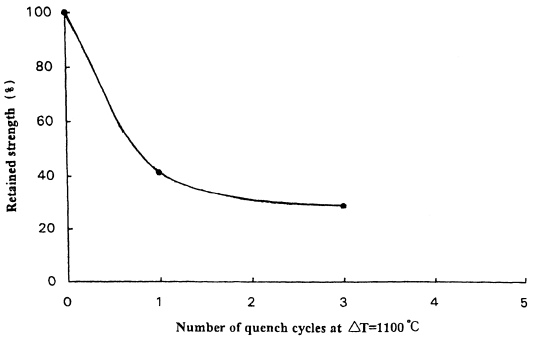

Fig. 5. Variation of percentage retained strength with the water quench cycle of castables containing 18 wt.% -30+10 mm top size aggregates with 35 wt.% -0.075 mm fines.

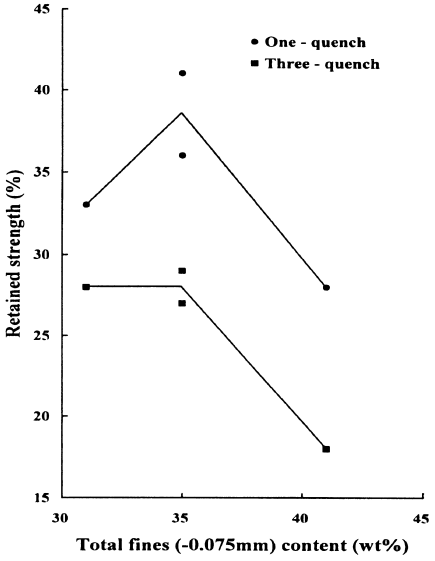

Fig. 6. Variation of percentage retained strength with the total fines content of castables.

particularly noticed that the castables containing 41 wt.% -0.075 mm fines have the lowest percentage retained strength after each quench test.

Field experience indicates that the Al_2O_3–spinel castables containing around 40 wt.% -0.075 mm fines for use in steel ladle linings are liable to serious spalling after around 35 heats, which resulted in a shortened life or a prematured failure. Normally the castables containing no more than 35 wt.% -0.075 mm fines should last at least 160 heats without gunning treatments in a secondary steelmaking environment at China Steel.

A careful study of the work of Homeny et al. [3] revealed that the total fines content of the gap-sized castables varied from 24.2 to 34.2 wt.% -0.075 mm fines, while that of the continuous-sized castables varied from 40.2 to 50.2 wt.% -0.075 mm fines; the gap-sized castables containing 34.2 wt.% -0.075 mm fines showed the best thermal shock damage resistance; and the thermal shock damage resistance of the continuous-sized

castables decreased with increasing wt.% -0.075 mm fines.

Two parameters R'''' and R_{st} [14,15] are often used to asses the thermal shock damage resistance of refractories as follows:

$$R'''' = \frac{E\gamma_{WOF}}{\sigma_f^2}$$

$$R_{st} = \left(\frac{\gamma_{WOF}}{\alpha^2 E}\right)^{\frac{1}{2}}$$

where E is Young's modulus, γ_{WOF} is work of fracture surface energy, σ_f is modulus of rupture and α is thermal expansion coefficient.

The validity of the parameters used to asses the thermal shock damage behavior of refractories has been amply verified [16–18]. Figs. 7 and 8 show the variation of percentage retained strength with R'''' and R_{st}. The magnitudes of percentage retained strength of castables can be linearly correlated with those of R'''' and R_{st}, which increase with an increase in the percentage of retained strength.

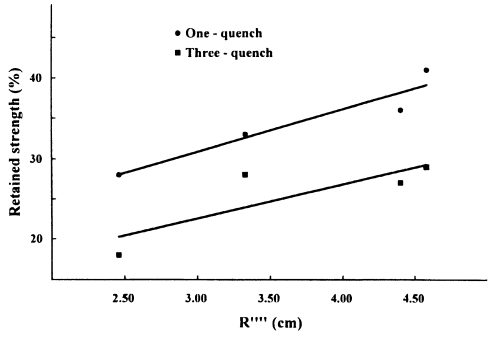

Fig. 7. Percentage retained strength of the castables subjected to water quench with $\Delta T = 1100°C$ as a function of the thermal shock damage resistance parameter, R''''.

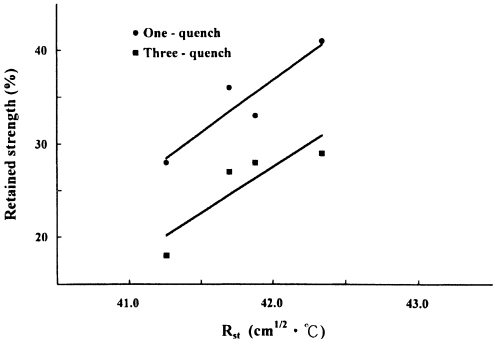

Fig. 8. Percentage retained strength of the castables subjected to water quench with $\Delta T = 1100°C$ as a function of the thermal shock damage resistance parameter, R_{st}.

4. Summary and conclusions

1. Castables containing 31–35 wt% -0.075 mm total fines have better thermal shock damage resistance than those containing 40 wt.% total fines, regardless of the size and amount of top size aggregates.
2. The thermal shock damage resistance parameters, R'''' and R_{st}, can be linearly correlated with the percentage retained strength of castables, which increases with an increase in the magnitudes of R'''' and R_{st}.
3. The experimentally observed work of fracture surface energy of castables increased with an increase in Young's modulus and modulus of rupture, while the notch beam fracture surface energy was dictated by the size and amount of top size aggregates and the larger size and amount of top size aggregates resulted in a higher magnitude of the notched beam fracture surface energy.

References

[1] P.P. Budnikov, The Technology of Ceramics and Refractories, MIT Press, Cambridge, MA, 1964, pp. 125–126.
[2] J.J. Uchno, R.C. Bradt, D.P.H. Hasselman, Fracture surface energies of magnesite refractories, Am. Ceram. Soc. Bull. 55 (1976) 665–668.
[3] J. Homeny, R.C. Bradt, Aggregate distribution effects on the mechanical properties and thermal shock behavior of model monolithic refractory systems, in: R.E. Fisher (Ed.), Advances in Ceramics, Vol. 13, New Development in Monolithic Refractories, Am. Ceram. Soc, Westerville, OH, 1985, pp. 110–130.
[4] H. Kubota, M. Sugawara, M. Harada, Y. Urita, M. Kataoka, K. Yamaguchi, Effect of coarse aggregates on thermal spalling resistance of refractory castables for steel ladle linings (size and amount of coarse aggregates part I), Taikabutsu 51 (1999) 266–274.
[5] H. Kubota, Y. Urita, M. Sugawara, M. Kotaoka, H. Yamashiro, Effect of coarse aggregates on thermal spalling resistance of refractory castables for steel ladle linings (size change of coarse aggregates part II), Taikabutsu 51 (1999) 316–325.
[6] JIS Refractories R2521, Refractories Manual '97, The Technichal Association of Refractories, Japan, 1997, pp. 372–385.
[7] D.R. Larson, J.A. Coppola, D.P.H. Hasselman, R.C. Bradt, Fracture toughness and spalling behavior of high-Al_2O_3 refractories, J. Am. Ceram. Soc. 57 (1974) 417–421.
[8] J. Homeny, T.R. Darroudi, R.C. Bradt, J-integral measurements of the fracture of 50% alumina refractories, J. Am. Ceram. Soc. 63 (1980) 326–331.
[9] Y.T. Chien, Y.C. Ko, High temperature fracture energy and thermal stress resistance parameters of bauxite brick, Am. Ceram. Soc. Bull. 64 (1985) 1017–1020.
[10] Refractories Handbook, The Technical Association of Refractories, Japan, 1998, pp. 86–87.
[11] T. Yamamura, Y. Kubota, T. Kaneshige, M. Nanba, Effect of spinel clinker composition on properties of alumina-spinel castable, Taikabutsu Overseas 13 (1993) 39–45.
[12] C.F. Chan, Y.C. Ko, Effect of CaO content on the hot strength of alumina-spinel castables in the temperature range of 1000 to 1500°C, J. Am. Ceram. Soc. 81 (1998) 2957–2960.
[13] Y.C. Ko, C.F. Chan, Effect of spinel content on hot strength of alumina-spinel castables in the temperature range 1000–1500°C, J. Eur. Ceram. Soc. 19 (1999) 2633–2639.

[14] D.P.H. Hasselman, Elastic energy at fracture and surface energy as design criteria for thermal shock, J. Am. Ceram. Soc. 46 (1963) 535–540.
[15] D.P.H. Hasselman, Unified theory of thermal shock fracture initiation and crack propagation in brittle ceramics, J. Am. Ceram. Soc. 52 (1969) 600–604.
[16] D.R. Larson, D.P.H. Hasselman, Comparative spalling behaviour of high-alumina refractories subjected to sudden heating and cooling, Trans. Brit. Ceram. Soc. 74 (1975) 59–65.
[17] D.P.H. Hasselaman, Role of fracture toughness in the spalling resistance of refractories, Bull. Soc. Franc. Ceram. 117 (1977) 19–30.
[18] J.H. Ainsworth, R.H. Herron, Thermal shock damage resistance of refractories, Am. Ceram. Soc. Bull. 53 (1974) 533–538.